PRINCIPLE OF A HIGH-SPEED CALCULATION FOR VIEW FACTOR AND SOLAR RADIATION BY COMPUTER GRAPHICS

K.Ikejima[1], A.Kaga[2] and A. Kondo[2]

[1] Advanced Knowledge Laboratory
Tokyo,Japan
[2] Division of Sustainable Energy and Environmental Engineering
Osaka University, Osaka, Japan

ABSTRACT

In this paper, we introduce a new calculation method of view factor and direct solar radiation, as a tecnique applicable in Computational Fluid Dynamics (CFD) analyses of thermal environment including the effect of thermal radiation. The method utilizes perspective and parallel projection images drawn with Computer Graphics (CG) technologies. The projection is applied to the three-dimensional models to two-dimensional digital images in order to calculate necessary factors for three-dimensional CFD analyses. In this paper, the principle and the procedure of the method is described and the accuracy is compared with existing methods. It is shown that the time saving of our new method is quite significant compared with commonly used methods.

INTRODUCTION

In thermal analyses, thermal and solar radiation often plays a significant role. It is also a very important factor in CFD analyses. In order to analyze thermal radiation between two surfaces, the view factor is necessary. The view factor is the ratio of the energy a body receives and the total energy emitted by a radiant body. In case of thermal analyses involving direct solar radiation, the identification of surface areas on which sunlight enters (irradiation area) is necessary.

View factors and irradiation areas are determined only by the geometry of a system analyzed and can be calculated analytically for a simple geometry. However, in case of including complicated shielding objects, the analyses become very difficult. Traditionally they are commonly calculated with Monte Carlo Simulation[1] and the accuracy of the method has been verified. For direct solar radiation analyses, rays are emitted from surface elements toward the sunlight direction to judge whether the ray is interrupted by obstacles. However, these methods are not practical in CFD analysis for complicated cases due to the calculation time required. We paid our attention to CG techniques which have been developed to process 3-dimensional geometric forms and to the fact that the graphic hardware has been highly optimized for high-speed transformation, and developed a new method to calculate view factors and irradiation areas using CG techniques. For view factor calculation, Pyramid Projection Method (PPM) which uses perspective images is proposed and for irradiation areas of direct solar radiation, parallel projection method is proposed. In this paper, the principle and the procedure of the method is described in detail. The time saving by the method and the accuracy are also discussed.

1.VIEW FACTOR CALCULATION WITH PERSPECTIVE IMAGES

1.1 View Factors and Piramid Projection

The view factor *dF* between the unit area at the origin O (view point) and an area *dS* located in three-dimensional space is calculated by the solid angle of dS and is given by equation (1).

$$dF = \frac{dS' \cos q}{p} \qquad \text{.... (1)}$$

where

dF: View factor between the unit area at the point O and dS
dS': Projection of dS on the surface of the hemisphere with unit radius
θ: Angle between the view line OA and z-axis

In order to calculate the view factor from perspective images, it is necessary to project the area dS' again to a plane. In this paper, a pentahedron (square pyramid) is used as a projection surface because of the simple relationship with orthogonal coordinate system and ease of calculation. This projection method has merits in the points of less surface numbers and same surface shapes compared with Hemi-Cube[2] method.

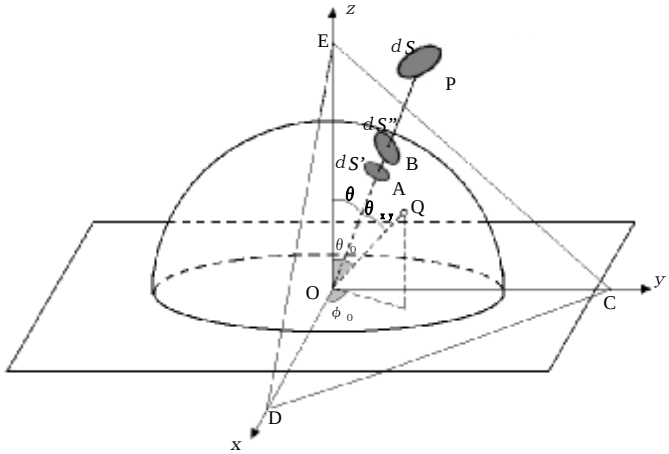

Fig. 1. Principle of Pyramid Projection Method

The projection method proposed here is named Pyramid Projection Method (PPM). As shown In Fig.1, the plane CDE which touches the hemisphere at the point Q(θ= π/4 and ϕ_0 = π/4) is chosen as one of the projection plane. The segment in the first quadrant of x-y-z coordinate is projected on the triangle plane CDE. Likewise, other quadrants is projected to other sides of the pentahedron.

The segment *dS''* in Fig.1 is the projection of the *dS'* on the plane CDE. The relationship between dS' and dS'' is given by Eq. (2). This equation shows that the view factor dF is given by projected area dS'' on the plane CDE and its location. Therefore, the view factor between the unit area on the bottom plane and segment dS in the three-dimentional space can be acquired by Eq. (2) using projected images.

$$dF = \frac{dS'' \cos q \cos^3 q_{xy}}{p} \qquad \ldots\ldots(2)$$

where,
θ_{xy}: Angle between view line OA and OQ in [rad].

1.2 Calculation Procedure

In case the view factor of dS given by Eq. (2) is calculated from a digital image, it is given by the sum of the view factor of each pixel which constitutes dS''. Therefore the view factor of every pixel on the projected image is calculated beforehand and prepared as a table. Next, the different RGB values are given to each mesh elements on the surface of the objects to be analyzed to identify the mesh element with which each pixel belongs. Then, a perspective projected image is drawn with CG, and the view factor of each pixel from the table is added for every different mesh element based on the color of each pixel.

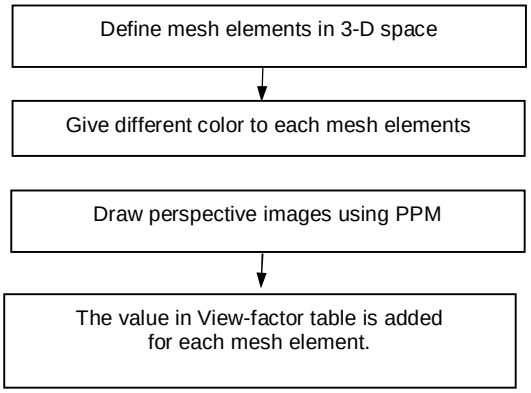

Fig.2. procedure for PPM

2. PARALLEL PROJECTION FOR SOLAR RADIATION

2.1 Parallel Projection

The solar rays landing earth's surface are considered to be parallel. In this paper, a method using CG to calculate direct solar radiation is proposed, and explained for an example of a sunny room shown in Fig.3.

We set horizontal (x) and vertical (y) axis on the window surface and z-axis normal to the window surface. The sun height h, and directional angle α are given by .Eqs. (3) and (4), and the view direction(-z') is coincided to the direction of sunlight.

$$\sin h = \sin j \sin d + \cos j \cos d \cos t \qquad \ldots\ldots(3)$$

$$\cos a = \frac{\sin h \sin j - \sin d}{\cos h \cos j} \qquad \ldots\ldots(4)$$

where, φ is the longitude, δ is the solar declination, t is the time angle. In a parallel projection with CG, a screen EFGH is placed normal to the view line (-z') as shown in Fig. 3.

Since the room space is the zone to be analyzed in this example, window area (strictly speaking the area extended by the dimension of the mesh element) is set to be the projected object. In Fig.3, four corners of the window

$$A(x_1, y_1, 0), B(-x_1, y_1, 0), C(-x_1, -y_1, 0), D(x_1, -y_1, 0)$$

is projected to

$$A'\left(x_1', y_1', z_1'\right), B'\left(-x_1', y_2', z_2'\right), C'\left(-x_1', -y_1', -z_1'\right), D'\left(x_1', -y_2', -z_2'\right)$$

in x'y'z' coordinate system by Eq. (5)

$$\begin{bmatrix} x' \\ y' \\ z' \\ 1 \end{bmatrix} = \begin{bmatrix} 1 & 0 & 0 & 0 \\ 0 & \cos -h & -\sin -h & 0 \\ 0 & \sin -h & \cos -h & 0 \\ 0 & 0 & 0 & 1 \end{bmatrix} \begin{bmatrix} \cos -a & 0 & \sin -a & 0 \\ 0 & 1 & 0 & 0 \\ -\sin -a & 0 & \cos -a & 0 \\ 0 & 0 & 0 & 1 \end{bmatrix} \begin{bmatrix} x \\ y \\ z \\ 1 \end{bmatrix} \quad \ldots(5)$$

Therefore, window surface ABCD is projected to parallelogram A'B'C'D' on the two-dimensional x'y' coordinate.

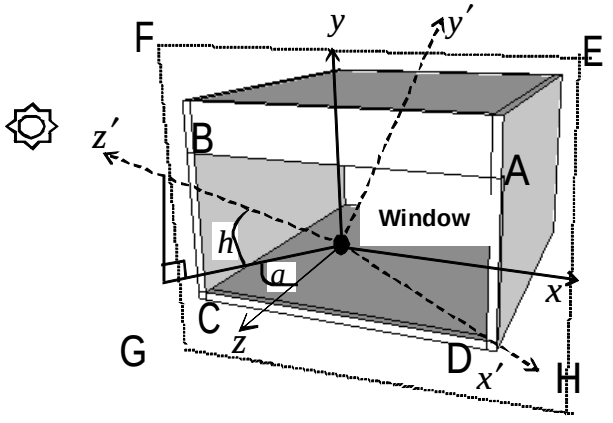

Fig. 3. Parallel projection for solar radiation

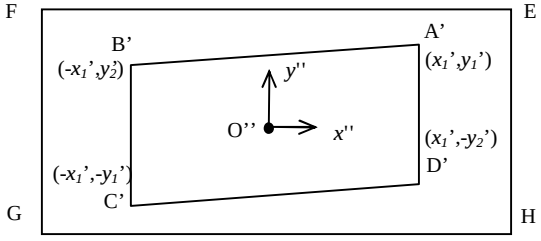

Fig. 4. Projection plane EFGH

2.2 Method to calculate solar radiation using parallel projection

Similar to 1.2, unique RBG value is given to the each mesh element on the surface of the walls and the floor of the room. Next, if required, furnitures, such as a desk and a chair, is installed in the room. Then parallel project from the direction of sunlight is drawn with CG. and the total number of pixels n_i which has the same color (i is the mesh element number) is counted for every mesh element . By comparing n_i with N_i which is the number of the pixels corresponding to a mesh element on the screen without any shield, we can judge whether a part of the mesh element is shielded. As described later, approximate value of N_i can be calculated also theoretically. The procedure is summarized in Fig.5.

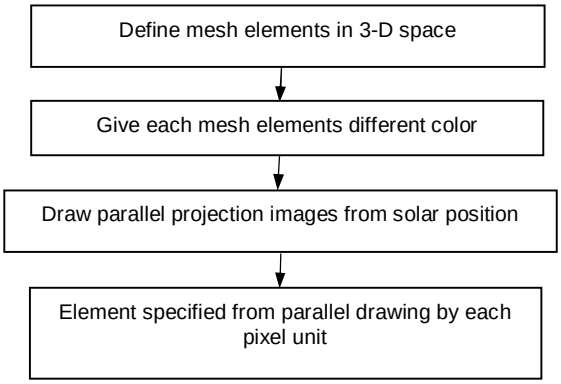

Fig.5. Procedure for solar radiation

The relative incoming flux, I_i ,which is defined as the ratio of incoming flux on a mesh element to the incoming flux on the unit area of a surface normal to the sunlight can be calculated by the following equations .

i) When $n_i = 0$ $I_i = 0$
ii) When $n_i = N_i$ $I_i = \beta_i A_0$
iii) When $n_i < N_i$ $I_i = \beta_i (n_i / N_i) A_0$

where, A_0 is the area of a surface element, β_i is the cosine of the normal vector and the solar ray vector described by Eq .(22) in the Appendix.

3. ERROR ANALYSIS

3-1 Error analysis for view factor calculation

The error analysis for the view factor calculation method is executed. The example model is a cube shown in Fig 6.

The three surfaces of the cube are divided to 5x5, 10x10, and 20x20 for the analysis. The result by PPM is compared with the result by Monte Carlo Method. The number of rays used for the Monte Carlo Method is 9 million, and the view factors obtained can be assumed to be accurate. The error err_i is defined by Eq.(6)

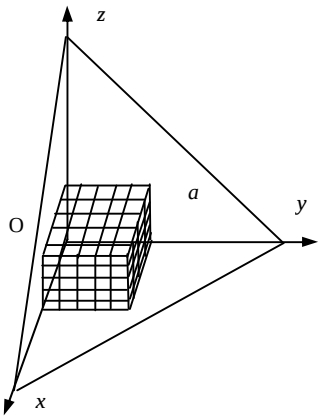

Fig.6. Error valuation model

$$err_i = VF_i - LVF_i \quad \text{.... (6)}$$

err_i : Error for mesh element i

VF_i : View factor by PPM

LVF_i : View factor by Monte Carlo Method

The absolute value of the error in view factor, $|err_i|$, is shown as a spatial distribution chart in Fig. 7. Three surfaces are divide to 10 x10 mesh elements and the resolutions of the perspective image are set to (a)160x120 pixels and (b) 640x480 pixels. Since the value of view factors near the bottom of the triangle becomes small, the absolute value of the error also becomes small.

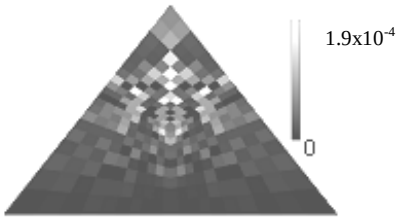

(a) Image resolution : 160x120 pix

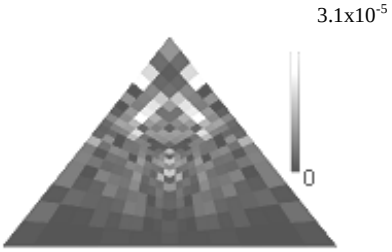

(b) Image resolution : 640x480 pix

Fig. 7 Error distribution of View factor
(Mesh dividing: 10x10)

The histogram of the errors in case perspective image resolution of (a)80x60 pixels and (b)2560x1920 pixels is shown in Fig.8..

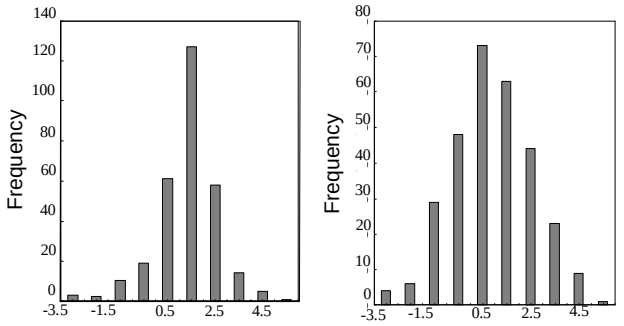

(a) Image resolution : 80x60 pix

(b) Image resolution : 2560x1920 pix

Fig. 8 Histogram of errors (mesh dividing: 10x10)

It is shown that the error err_i distributes around its average value zero, and decreases with the image resolution increases.

Furthermore, the theoretical value of the standard deviation of the error, σ_{th} is derived as Eq.(7) by assuming the error is purely due to the quantizing error[3].

$$s_{th} = \frac{n_T^{-3/4} n_D^{-1/4}}{\sqrt{48}} \quad \text{.... (7)}$$

where,

n_D: Total number of mesh elements on the projected image

n_T: Number of pixels on the projected image [pixels]

The comparison of the standard deviation of measured errors with Eq. (7) is shown in Fig.9. Fig. 9 shows that the Eq. (7) is applicable to estimate the order of the magnitude of the error.

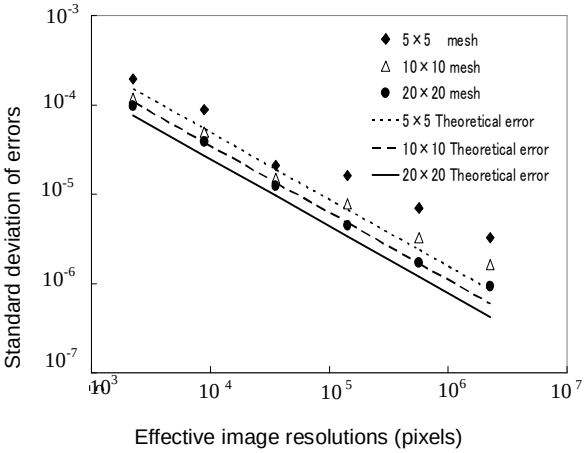

Fig. 9 Observed and theoretical errors

3-2. Error analysis on solar radiation calculation

As shown in 2.2, calculation of incoming flux does not include any error for cases i) and ii). However, for the case iii), as shown in Fig. 10, there appears a line of shadow border on a mesh element and an error due to the quantization to express the irradiation area with the number of pixels n_i .

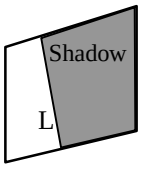

Fig. 10. Divided mesh element

The error for the case iii) is define as;

$$E_i = b_i (r_i - r_{i,true}) \quad \text{.....(8)}$$

$$r_i = \frac{n_i}{N_i} \quad \text{.....(9)}$$

$r_{i\,true}$: true value of r_i

E_i is the error included in the calculated incoming flux relative to the incoming flux when the element is exposed to the sunlight which incidences perpendicularly.

According to Deguchi [4] , the average value of the theoretical error included in approximating an area with thier pixel numbers on a digital image is zero and the variance is given by

$$S = \frac{1}{12}\frac{M}{N^4} \quad \text{.... (10)}$$

Here, M is the number of pixels on the border line segment L shown in Fig.10, and N is the resolution of projection image and $N=N_{Wx}$ (pixel numbers corresponding to the width of the window on the image) in case the coordinates are expressed by nondimensional length divided by the window width.

Although the length of L varies with cases, their average is assumed to the half of their maximum length L_{max} (longer diagonal line of parallelogram image) here.

$$L_{ave} = \frac{1}{2} L_{\max} \quad \text{.... (11)}$$

In this case, M is given by

$$M = L_{ave} N_{Wx} \quad \text{.... (12)}$$

and, the theoretical value of the standard deviation of the errors in area estimation is given by

$$s_{A,th} = \sqrt{\frac{L_{\max}}{24 N_{Wx}^3}} \quad \text{.....(13)}$$

The theoretical value of the standard deviation of E_i in Eq.(8) is

$$s_{E,th} = \frac{s_{A,th}}{A_0} \quad \text{.... (14)}$$

The incoming flux error defined by Eq. (8) is estimated for a room model shown in Fig. 11 and compared with the result with commonly used ray emission method.

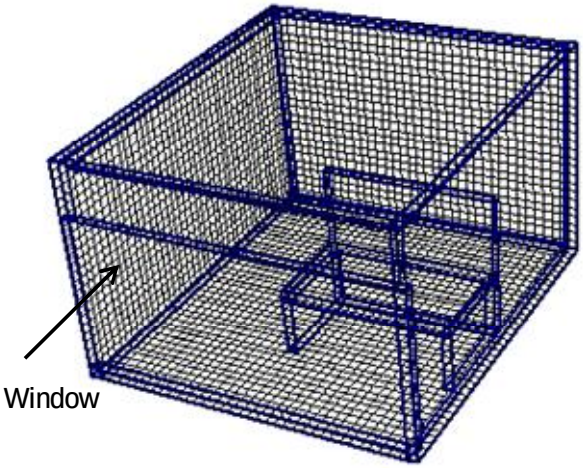

Fig. 11 Room model and mesh division

The dimension of the room model is 3.6m in width, 4m in depth, and 2.4m in height, and has a window on the south side wall with the height of 1.7m. The walls and a floor are divided to the mesh elements of 0.1m x 0.1m. Fig. 12 shows the parallel projection on December 22th on the winter solstice at 14:00 in Tokyo(The figure is rotated in order to prevent the systematic error in area calculation of mesh elements).

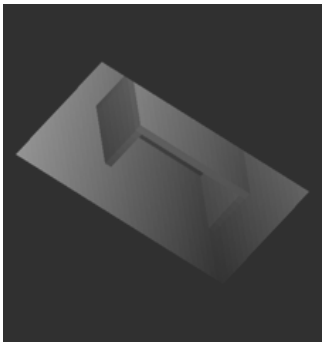

Fig. 12 Parallel projection image

Fig.13 shows the histogram of errors defined by Eq.(8) for the resolution of projection image of 500x500 pix and 2000x2000 pix. Fig. 13 shows that the error distributes around its average value zero, and decreases with the image resolution increases. This characteristics agrees with the theory described above.

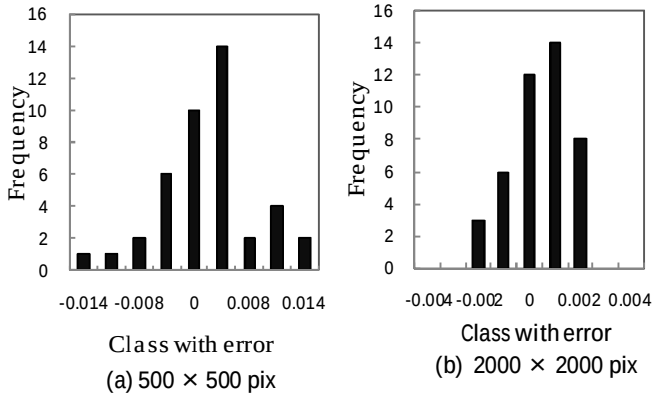

Fig.13 Histogram of error distribution

The magnitude of the standard deviation of the error is compared with the theoretical one given by Eq.(14) and shown in Fig.14. The observed standard deviation of the errors is the average obtained on the floor and walls. The observed error has the magnitude of less than 10 times of theoretical one and the main source of the error is considered the quantization error.

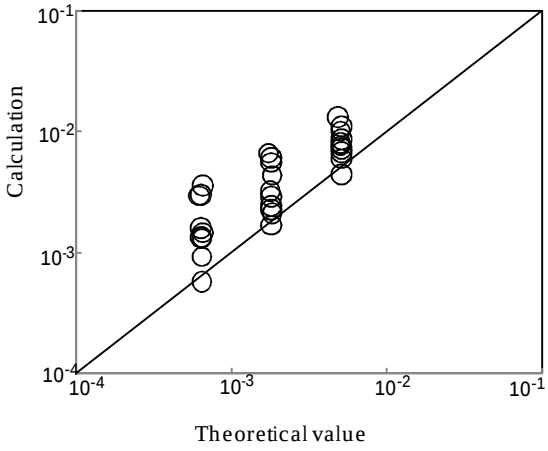

Fig. 14 Comparison between observed and theoretical error

4. COMPARISON OF CALCULATION TIME

Fig. 15 shows the relation between calculation time and the magnitude of the standard deviation of the error for PPM and Monte Carlo method. Compared with Monte Carlo method, the calculation time of PPM for the same error is about 10^{-4} and the high performance in computation time of the new method is verified.

Fig. 16 shows the relation between calculation time and the magnitude of the standard deviation of the error for CG method and a traditional ray emission method. Compared with the traditional method, the new one has about 10^3 to 10^4 times higher performance.

CONCLUSION

In this paper, a new calculation method of view factor and direct solar radiation, using digital images drawn with CG is proposed. The accuracy and calculation

speed improvement of the method are also discussed. The main source of the error is considered to the quantization in image drawing process and it is insignificant for most usages. The new method has sufficient advantage compared with the traditional ray emission methods like Monte Carlo method.

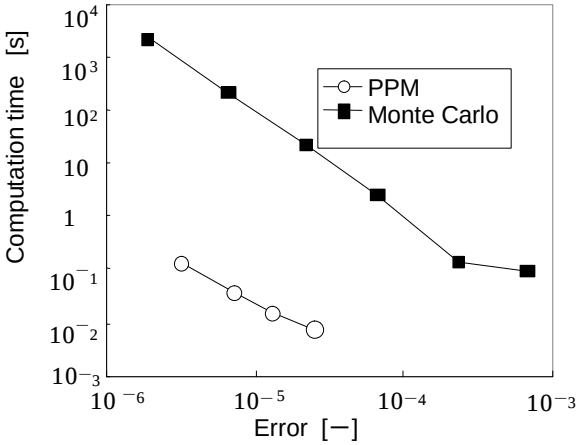

Fig.15 Error and the computation time

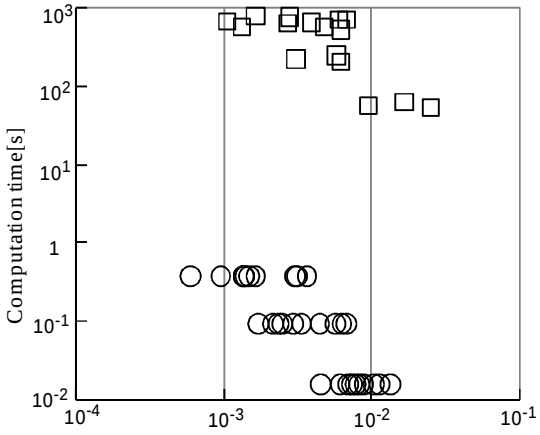

Fig.16 Error and the computation time

APPENDICES

The theoretical calculation value of L_{max} and β

The point (x,y,x) in a real space is projected to the point (x',y') on a projection plane as follows.

$$x' = C_a x + S_a z \quad \text{.... (15)}$$

$$y' = -S_h S_a x + C_h y + S_h C_a z \quad \text{.... (16)}$$

$$C_a = \cos(-a), \qquad S_a = \sin(-a),$$

$$C_h = \cos(-h), \qquad S_h = \sin(-h), \quad \text{.... (17)}$$

A square mesh element of size *d* is projected on the walls and a floor as shown in Fig.17.

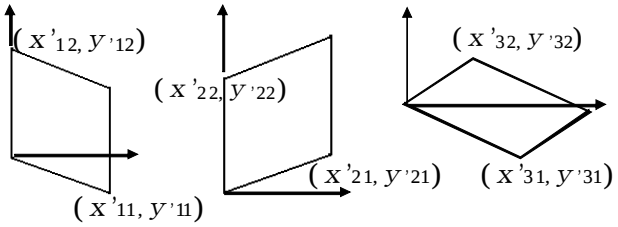

Fig. 17 Coordinates on projection

$$x'_{11} = C_a d, \qquad y'_{11} = S_h S_a d$$

$$x'_{12} = 0, \qquad y'_{12} = C_h d$$

$$x'_{21} = -S_a d, \qquad y'_{21} = -S_h C_a d \quad \text{.... (18)}$$

$$x'_{22} = 0, \qquad y'_{22} = C_h d \quad \text{.... (19)}$$

$$x'_{31} = C_a d, \qquad y'_{31} = S_h S_a d$$

$$x'_{32} = S_a d, \qquad y'_{32} = -S_h C_a d \quad \text{.... (20)}$$

Area of mesh element image is

$$A_j = \left| x'_{j1} y'_{j2} - y'_{j1} x'_{j2} \right| \quad \text{.... (21)}$$

(j =1,2,3)

The cosine of the angle between outward normal vector sunlight vector is

$$b_j = \frac{A_j}{d^2} \quad \text{.... (22)}$$

The maximum Length of diagonal line is

$$L_{\max,j} = \max\left\{L_{1j}, L_{2j}\right\} \quad \text{.... (23)}$$

$$L_{1j} = \sqrt{\left(x'_{ji} + x'_{j2}\right)^2 + \left(y'_{j1} + y'_{j2}\right)^2}$$

$$L_{2j} = \sqrt{\left(x'_{ji} - x'_{j2}\right)^2 + \left(y'_{j1} - y'_{j2}\right)^2}$$

.REFERENCES

1. J. R. Howell and M. Perlmutter:Monte Carlo Solution of Thermal Transfer Through Radiant Media Between Gray Walls,Trans. ASME,Vol. 86 (1964) pp.116-122
2. F. C. Michael and P. G. Don:The Hemi-cube: A Radiosity Solution for Complex Environments,ACM ComputerGraphics (SIGGRAPH),Vol. 19, No. 3 (1985) pp.31-40
3. Kenji Shiotani, Akikazu Kaga, Akira Kondo, Yoshio Inoue, Wookhyun Yeo: Calculation method of heat radiation using computer graphics technique, ED.01, CDROM Proceedings of Sixth KSME-JSME Thermal and Fluids Engineering Conference(Korea),2004-12
4. Koichiro Deguchi: About the area measurement with pixel numbers in digital imaging, Journal of the Society of Instrument and Control Engineers, 27-2 (1991), pp.227-229. (in Japanese)